BIOCHEMISTRY
including biophysical chemistry & molecular biology

Accelerated Publication

pubs.acs.org/biochemistry

Motifs Q and I Are Required for ATP Hydrolysis but Not for ATP Binding in SWI2/SNF2 Proteins

Macmillan Nongkhlaw,† Meghna Gupta, Sneha Sudha Komath, and Rohini Muthuswami*

School of Life Sciences, Jawaharlal Nehru University, New Delhi 110067, India

Supporting Information

ABSTRACT: Active DNA-dependent ATPase A Domain (ADAAD) is a SWI2/SNF2 protein that hydrolyzes ATP in the presence of stem−loop DNA that contains both double-stranded and single-stranded regions. ADAAD possesses the seven helicase motifs that are a characteristic feature of all the SWI2/SNF2 proteins present in yeast as well as mammalian cells. In addition, these proteins also possess the Q motif ∼17 nucleotides upstream of motif I. Using site-directed mutagenesis, we have sought to define the role of motifs Q and I in ATP hydrolysis mediated by ADAAD. We show that in ADAAD both motifs Q and I are required for ATP catalysis but not for ATP binding. In addition, the conserved glutamine present in motif Q also dictates the catalytic rate. The ability of the conserved glutamine present in motif Q to dictate the catalytic rate has not been observed in helicases. Further, the SWI2/SNF2 proteins contain a conserved glutamine, one amino acid residue downstream of motif I. This conserved glutamine, Q244 in ADAAD, also directs the rate of catalysis but is not required either for hydrolysis or for ligand binding. Finally, we show that the adenine moiety of ATP is sufficient for interaction with SWI2/SNF2 proteins. The γ-phosphate of ATP is required for inducing the conformational change that leads to ATPase activity. Thus, the SWI2/SNF2 proteins despite sequence conservation with helicases appear to behave in a manner distinct from that of the helicases.

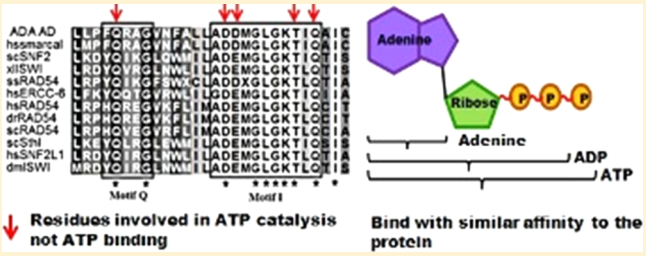

The SWI2/SNF2 family of proteins plays a critical role in transcription, repair, replication, and recombination. The ATPase activity of these proteins is used for remodeling chromatin during replication, repair, transcription, recombination, and histone variant exchange.[1−4] The presence of the seven helicase motifs is a characteristic feature of all SWI2/SNF2 proteins.[5] In addition, the SWI2/SNF2 proteins also contain the recently identified Q motif.[6]

Structural studies of the SWI2/SNF2 proteins, SsRad54cd, zebrafish Rad54, and RapA, have shown that the helicase motifs are arranged in two RecA-like domains.[7−9] Motifs I, Ia, II, and III are present in the N-terminal domain (subdomain IA or 2A), and motifs IV, V, and VI are present in the C-terminal domain (subdomain 1B or 2B).[7,8] A comparison of the crystal structure of *Solfolobus solfataricus* SsRad54cd and zebrafish Rad54cd with that of *Thermotoga maritima* RecG helicase indicates that the two RecA-like domains are equivalent to the DEXX box region that contains the conserved helicase motifs.[10]

The role of the individual motifs has been elucidated in helicases. For example, the conserved lysine of the GKT box has been shown to be important for ATP hydrolysis.[11,12] In some helicases, this conserved lysine of the GKT box has been shown to be required for ATP binding, too, though this is not universally true.[13] Similarly, the Q motif has been shown to be important for catalysis and has a possible role in nucleotide recognition in DEAD box helicases (eIF4A and Ded1) and SF1 helicase UvrD.[6,11,14] Motif III has been shown to be an ATP sensor, while motif VI has been shown to be critical for ATP hydrolysis.[15−18]

Functional characterization of the helicase motifs has been conducted in some members of the SWI2/SNF2 family. Mutation of the conserved lysine to alanine or arginine in the GKT box (K798R in Snf2 and Brg1 and K501R in Sth1) has been shown to abolish the ATPase activity of Snf2, Sth1, and Brg1.[19−21] Similarly, a study by Richmond and Peterson in yeast SNF2 protein has shown that mutation of the lysine to alanine in the GKT box, aspartate to alanine or glutamate in the DEXX box, arginine to alanine in motif IV (R994A), and arginine to lysine in motif VI (R1196K) and deletion of the entire motif V (ΔSTRAGGLG) affected the ability of the proteins to complement the transcriptional defect due to deletion of the *SWI2* gene.[22]

Genetic analysis has also indicted the importance of the helicase motifs. Mutations in the ATPase domain of SMARCAL1 have been linked to Schimke-immunosseous dysplasia.[23] Mutations in the ATPase domain Brg1 and Brm have been linked to many cancers. Further, recent studies have shown that mutation of the conserved lysine in the GKT box (K755R) of SMARCA2 (Brm) results in Nicolaides-Baraitser

Received: September 20, 2011
Revised: April 11, 2012
Accepted: April 17, 2012
Published: April 17, 2012

A

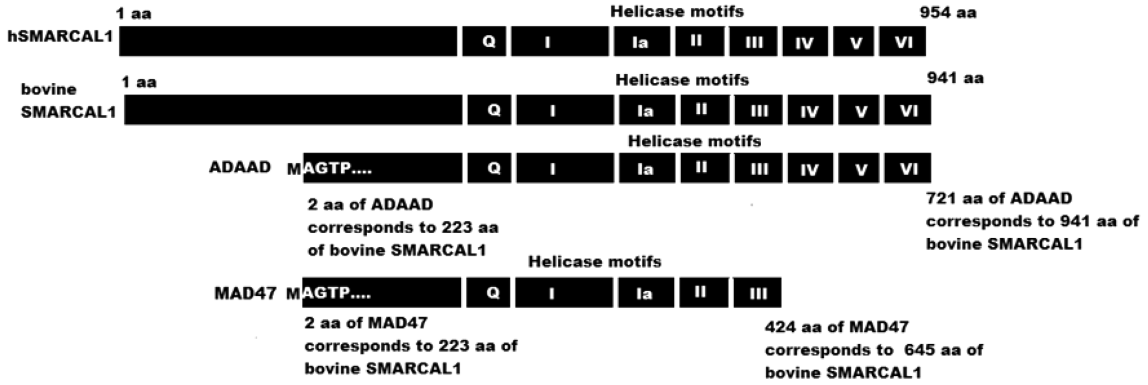

B.

MOTIFS	Conserved amino acids	hSMARCAL1	ADAAD
Q	Q	440 aa	217 aa
I	LLLADDMGLGKT	454-465 aa	230-242 aa
Ia	PSSVR	286-290 aa	263-267 aa
II	DESH	549-552 aa	326-329 aa
III	SGTP	579-582 aa	355-358 aa
IV	FAHH	731-734 aa	507-510 aa
V	SITAAN	783-788 aa	558-563 aa
VI	HRIGQ	819-823 aa	594-598 aa

C.

ADAAD	bSMARCAL1	hSMARCAL1
Q217	Q438	Q440
D235	D456	D458
D236	D457	D459
T242	T463	T465
Q244	Q465	Q467

Figure 1. (A) Schematic representation of human SMARCAL1 (hSMARCAL1), bovine SMARCAL1, ADAAD, and MAD47. hSMARCAL1 is 954 amino acids long, while bovine SMARCAL1 is 941 amino acids long. ADAAD is an 82 kDa proteolytic fragment derived from bovine SMARCAL1. The sequence starts from amino acid 223 (alanine residue) and ends at amino acid 941 of bovine SMARCAL1. A methionine was incorporated ahead of alanine 223. In numbering, methionine was counted as 1 and alanine was counted as 2. Thus, the amino acid 2 of ADAAD corresponds to amino acid 223 of bovine SMARCAL1. MAD47 starts from amino acid 223 and ends at amino acid 424 of bovine SMARCAL1. (B) Sequences of the conserved motifs present in SMARCAL1. We have provided the amino acid numbers in human SMARCAL1 and ADAAD. For ADAAD numbering, we have counted alanine 223 of bovine SMARCAL1 as the amino acid 2 of ADAAD. (C) List of amino acids analyzed in this paper.

syndrome, indicating the importance of this conserved residue.[24]

However, the roles of motif Q as well as that of motif I with respect to ATP binding and catalysis in SWI2/SNF2 proteins have not yet been addressed. Further, it is pertinent to note that motif I of the SWI2/SNF2 proteins differs from that of the helicases by the presence of two acidic residues upstream of the GKT motif. The function of these two aspartates has not yet been elucidated.

Therefore, in this paper, we have endeavored to address the role of motifs Q and I in ATP hydrolysis mediated by these proteins. We have used Active DNA-dependent ATPase A Domian (ADAAD) as the model system. ADAAD is an 82 kDa proteolytic fragment of SMARCAL1.[25−28] A schematic representation of human SMARCAL1, bovine SMARCAL1, and ADAAD along with the motifs is given in Figure 1. Previously, we have shown that both ATP and DNA can interact with ADAAD in the absence of the other ligand.[29] Binding of either ligand induces a conformational change that allows the other ligand to bind with a higher affinity.[29] In this paper, we seek to elucidate the role of motifs Q and I. We show that motifs Q and I are required only for ATP hydrolysis.

dx.doi.org/10.1021/bi2014757 | *Biochemistry* 2012, 51, 3711−3722

Further, we show that the adenine moiety of ATP is sufficient for the interaction. The terminal γ-phosphate of ATP is critical for inducing the conformational change required for ATP hydrolysis. This mechanism is reminiscent of ATP hydrolysis mediated by P-type ATPases, suggesting that the SWI2/SNF2 proteins, though classified as helicases, might be binding ATP in a manner different from that of helicases.

EXPERIMENTAL PROCEDURES

Chemicals. All chemicals were of analytical grade and were purchased from either Merck or Sigma-Aldrich. The primers for making the site-directed mutants and deletion constructs were synthesized by Sigma-Aldrich. The stem−loop DNA (slDNA, 5′-GCGCAATTGCGCTCGACGATTTTTTAGCG-CAATTGCGC-3′) used for ATPase assays as well as binding assays was also synthesized by Sigma-Aldrich. TNP-ATP was purchased from Sigma-Aldrich.

Creating Deletion Constructs and Site-Directed Mutants. pMN82, which is a pGEX-6P-2 plasmid containing the ADAAD gene, was used as the template for creating deletion and site-directed mutants. MAD47 containing only motifs Q, I, Ia, II, and III was created by polymerase chain reaction (PCR) amplification of pMN82 using primers listed in Table 1 of the Supporting Information. Site-directed mutants were made by PCR amplification using the mutagenic primers and conditions listed in Tables 1 and 2 of the Supporting Information, respectively. The PCR reaction mixture contained 0.2 μM dNTPs, each primer at 200 μM, 1.5 mM $MgSO_4$, 1× high-fidelity buffer (MBI Fermentas), and 1 unit of high-fidelity PCR enzyme mix (25 μL reaction volume). After amplification, the parental plasmid was digested with DpnI at 37 °C for 8 h (MBI Fermentas), and *Escherichia coli* cells were transformed with 8−10 μL of the reaction mix. The incorporation of the desired mutation in the transformant was confirmed by sequencing.

Protein Expression and Purification. pMN82 encoding ADAAD and the plasmids encoding the site-directed mutants and the deletion constructs were expressed as GST-tagged proteins in BL21(DE3) cells. For purification, a single colony was inoculated into 10 mL of LB containing 100 μg/mL ampicillin. The cells were grown for 16 h, and a 1% (v/v) inoculum was added to 250 mL of sterilized LB medium containing 100 μg/mL ampicillin. The cells were grown at 37 °C until OD_{600} reached 0.5. The cells were cooled to 16 °C until OD_{600} reached 0.8. The cells were induced by the addition of 0.5 mM IPTG and allowed to grow for 16 h at 16 °C. After the cells had been harvested, the cell pellet (∼10 g) was resuspended in 100 mL of lysis buffer containing 50 mM Tris-HCl (pH 8.0), 150 mM NaCl, 150 mM $MgCl_2$, 0.1% (v/v) Triton X-114, 0.2 mg/mL lysozyme, 10 mM β-mercaptoethanol, and 0.5 mM PMSF. The cells were homogenized and incubated for 1 h at 4 °C. This was followed by sonication (15 s on and 45 s off; five cycles), and the lysate was clarified by centrifugation at 12000 rpm for 30 min at 4 °C. To the supernatant was added 60% (w/v) ammonium sulfate to precipitate the proteins. The precipitate was harvested by centrifugation at 10000 rpm for 10 min at 4 °C. The protein pellet was resuspended in the buffer containing 50 mM Tris-HCl (pH 8.0), 2 M NaCl, 150 mM $MgCl_2$, and 5 mM β-mercaptoethanol and centrifuged at 40000 rpm for 2 h at 4 °C. After centrifugation, the supernatant was dialyzed against the buffer containing 50 mM Tris-HCl (pH 8.0), 150 mM NaCl, 150 mM $MgCl_2$, and 5 mM β-mercaptoethanol until the conductivity of the supernatant was the same as that of the dialysis buffer. The dialysate was loaded onto 1 mL glutathione−agarose beads (GE Healthcare) pre-equilibrated with dialysis buffer. The protein was eluted by incubating the protein bound to glutathione beads with 1−2 mL of cleavage buffer containing PreScission protease (GE Healthcare). The contaminating GroEL proteins were removed using a DEAE-Sepharose column.

Cloning and Overexpression of Sth1. The Sth1 gene was amplified from *Saccharomyces cerevisiae* genomic DNA using the forward primer (5′-CGCGAGAATTCATGGTT-CAAATTAGAAGCAAAGTTATTG-3′) and the reverse primer (5′-CGCGACTCGAGCGAAGAGTGTTCCTTGAACC-3′). The PCR conditions used for amplification were 94 °C for 5 min for initial denaturation followed by 30 cycles of 94 °C for 45 s, 44 °C for 30 s, and 72 °C for 3 min and a final extension for 10 min at 72 °C. The amplified product was restricted with BamHI and XhoI and cloned into vector pET21c(+). The sequence was verified by DNA sequencing. BL21(DE3) cells were transformed with the plasmid containing the Sth1 gene. Cells were induced with 1 mM IPTG and allowed to grow at 16 °C for 4 h before being harvested. Analysis of the lysed cells using sodium dodecyl sulfate−polyacrylamide gel electrophoresis (SDS−PAGE) showed the expression of the expected 124 kDa protein.

Purification of Sth1. A single colony of the transformed cell was inoculated into 10 mL of LB containing 100 μg/mL ampicillin and grown for 16 h at 37 °C; 1% (v/v) of the primary inoculum was transferred to fresh LB medium containing ampicillin. Cells were grown to an optical density of 0.5 before being induced with 1 mM IPTG. Cells were grown at 16 °C for 4 h postinduction and harvested by centrifugation at 5000 rpm for 10 min at 4 °C. Cells were incubated in lysis buffer containing 50 mM Tris-HCl (pH 8.0), 50 mM NaCl, 150 mM $MgCl_2$, 5% (v/v) glycerol, 1 mM β-mercaptoethanol, 0.5 mM PMSF, and 0.1 mg/mL lysozyme for 1 h at 4 °C and lysed by sonication (15 s on and 45 s off; five cycles). The cell lysate was clarified by centrifugation at 12000 rpm for 30 min at 4 °C, and the supernatant was loaded onto Ni^{2+}-NTA agarose beads (Qiagen) pre-equilibrated in equilibration buffer containing 50 mM Tris-HCl (pH 8.0), 50 mM NaCl, 150 mM $MgCl_2$, 5% (v/v) glycerol, and 1 mM β-mercaptoethanol. The column was washed with equilibration buffer, and the bound protein was eluted with imidazole. Imidazole was removed prior to analysis by dialyzing the protein against buffer containing 50 mM Tris-HCl (pH 8.0), 100 mM NaCl, 30% (v/v) glycerol, 1 mM β-mercaptoethanol, and 0.5 mM PMSF.

ATPase Assays. The ATPase activity was measured using either colorimetric estimation of phosphate released or coupled NADH oxidation assays.

Estimation of the Amount of Phosphate Released after ATP Hydrolysis. The ATPase activity of the proteins was determined by measuring the amount of phosphate released using a combination of a modified King's method[30] and the micro assay described by Gawronski et al.[31] Briefly, ADAAD was incubated with 10 nM slDNA and 2 mM ATP in buffer containing 50 mM Tris-SO_4 (pH 7.5), 5 mM β-mercaptoethanol, 1 mM $MgSO_4$, 2 mM phosphoenolpuryvate, and 150 μg/mL pyruvate kinase in a 50 μL reaction volume. The reaction mixture was incubated for 1 h at 37 °C. The amount of phosphate released was estimated by adding solution E that contains two parts of solution A (2% L-ascorbic acid in 1

Table 1. Comparison of K_d Values of Mutants with Respect to the Wild-Type Protein[a]

	K_d (M)			
	ATP	slDNA	ATP in the presence of slDNA	slDNA in the presence of ATP
wild type	$(1.5 \pm 0.1) \times 10^{-6}$	$(3.8 \pm 0.8) \times 10^{-9}$	$(0.14 \pm 0.02) \times 10^{-6}$	$(0.8 \pm 0.03) \times 10^{-9}$
MAD47	$(0.8 \pm 0.3) \times 10^{-6}$	$(7.6 \pm 0.07) \times 10^{-9}$	$(0.16 \pm 0.03) \times 10^{-6}$	$(0.7 \pm 0.2) \times 10^{-9}$
Q217A	$(0.7 \pm 0.2) \times 10^{-6}$	$(7.0 \pm 1.0) \times 10^{-9}$	$(0.1 \pm 0.01) \times 10^{-6}$	$(1.1 \pm 0.01) \times 10^{-9}$
Q217N	$(1.3 \pm 0.3) \times 10^{-6}$	$(7.2 \pm 1.3) \times 10^{-9}$	$(0.26 \pm 0.02) \times 10^{-6}$	$(1.5 \pm 0.01) \times 10^{-9}$
D235A	$(0.6 \pm 0.1) \times 10^{-6}$	$(4.3 \pm 0.4) \times 10^{-9}$	$(0.25 \pm 0.01) \times 10^{-6}$	$(1.3 \pm 0.7) \times 10^{-9}$
D236A	$(1.4 \pm 0.1) \times 10^{-6}$	$(5.8 \pm 0.03) \times 10^{-9}$	$(0.14 \pm 0.02) \times 10^{-6}$	$(0.7 \pm 0.01) \times 10^{-9}$
T242A	$(1.4 \pm 0.1) \times 10^{-6}$	$(9.2 \pm 0.5) \times 10^{-9}$	$(0.14 \pm 0.02) \times 10^{-6}$	$(0.8 \pm 0.01) \times 10^{-9}$
Q244A	$(1.1 \pm 0.09) \times 10^{-6}$	$(9.5 \pm 1.3) \times 10^{-9}$	$(0.16 \pm 0.02) \times 10^{-6}$	$(1.1 \pm 0.02) \times 10^{-9}$

[a] K_d values were calculated using a one-site saturation model. Each value was verified by at least two independent experiments with each experiment conducted in duplicate.

N HCl) and one part of solution C (2% ammonium molybdate in water). The color development was stopped by adding solution F [2% (w/v) sodium citrate tri basic in 2% (v/v) acetic acid]. The absorbance was recorded at 655 nm, and the specific activity was calculated as nanomoles of P_i released per minute per milligram of protein.

To determine whether adenine could inhibit the ATPase activity, ADAAD (0.21 μM) was incubated with 10 nM slDNA and 1 mM ATP in buffer containing 50 mM Tris-SO_4 (pH 7.5), 5 mM β-mercaptoethanol, and 1 mM $MgSO_4$ in the absence or presence of 2.5 mM adenine. The regeneration system was not used in the inhibition assay, and the amount of phosphate released was measured as described above.

Estimation of ATP Hydrolysis Using the Coupled NADH Oxidation Reaction. The kinetic studies of the protein were conducted by coupling ATP hydrolysis to NADH oxidation.[28] Briefly, 1.4 μg (68 nM, 176 nmol/250 μL reaction volume) of protein was incubated with different concentrations of slDNA in the presence of REG buffer containing 50 mM Tris-SO_4 (pH 7.5), 5 mM β-mercaptoethanol, 1 mM $MgSO_4$, 150 μg/mL pyruvate kinase, and 10 mM phosphoenolpyruvate in a 250 μL reaction volume. ATP and NADH were added to final concentrations of 2 mM and 0.1 mg/mL, respectively. The reaction mixture was incubated for 40 min at 37 °C. The change in absorbance was recorded at 340 nm, and the concentration of NADH oxidized was calculated using a molar extinction coefficient of NADH of 6.3 mM^{-1}.

Calculation of K_{DNA} and V_{DNA}. The data obtained from ATPase assays were analyzed with the equation

$$v = V_{DNA}[S]/K_{DNA} + [S]$$

where v is the rate of ATP hydrolysis, K_{DNA} is the apparent dissociation constant for DNA, V_{DNA} is the apparent maximal rate of ATP hydrolysis, and [S] is the concentration of DNA. As the DNA is not the substrate in the true sense, the terms K_{DNA} and V_{DNA} were used to describe K_m and V_{max}, respectively, for the reaction.[28]

Fluorescence Measurement. Fluorescence studies using tryptophan specific excitation were conducted as described in ref 29. The concentration of ADAAD used for fluorescence studies was 0.48 μM. The concentration of Sth1 used for fluorescence studies was 0.32 μM. The excitation wavelength was 295 nm, and the emission wavelength was 340 nm. The slit widths were 5 and 10 nm, respectively. The spectra obtained were corrected for dilution. In all the experiments, the inner filter effect was negligible. The data obtained were fit to a one-site saturation model, where it is assumed that there is one site for the interaction of the ligand with the protein. The K_d was calculated using the equation

$$\Delta F/F_o = B_{max}[L]/(K_d + [L])$$

where B_{max} is the maximal binding, [L] is the ligand concentration, and K_d is the dissociation constant. The K_d values calculated by this method are listed in Table 1. The K_d was also calculated using double-reciprocal plots, and the values are listed in Table 3 of the Supporting Information.

Fluorescence Quenching Studies. Acrylamide was used as a quencher to identify the populations of accessible tryptophans in the protein. In these studies, 0.37 μM protein was titrated with increasing concentrations of acrylamide and the change in fluorescence emission intensity was monitored at 340 nm upon excitation at 295 nm. The excitation and emission slit widths were 5 and 10 nm, respectively.

Stern–Volmer Plots. Stern–Volmer and modified Stern–Volmer plots were used to determine the population of tryptophan residues accessible to acrylamide. The recorded fluorescence intensities were used to create Stern–Volmer plots of F_o/F_c versus [Q] according to the equation $F_o/F_c = 1 + K_{SV}[Q]$, where F_o is the initial fluorescence intensity, F_c is the corrected fluorescence intensity, [Q] is the quencher concentration, and K_{SV} is the Stern–Volmer quenching constant.

To calculate the fraction of accessible tryptophans (f_a) as well as the association constant (K_a), we used modified Stern–Volmer plots of $F_o/\Delta F$ versus $[Q]^{-1}$ according to the equation $F_o/\Delta F = f_a^{-1} + K_a f_a [Q]^{-1}$.

Circular Dichroism (CD) Spectroscopy. Far UV CD spectra were recorded using Chirascan (Applied Photophysics) in a 1 mm cuvette. The recordings were made in buffer containing 20 mM Tris-HCl (pH 7.5), 100 mM NaCl, 1 mM EDTA, 1 mM $MgCl_2$, and 1 mM dithiothreitol. In these reactions, 0.1 mg/mL proteins, 20 μM nucleotide (ATP, ADP, or adenine), and 2 μM slDNA were used. The spectra obtained were corrected for buffer, dilution, and the ligands that were added. The CD spectra obtained in millidegrees were converted to mean residue ellipticity using the formula $[\theta] = (S \times mRw)/(10cl)$, where S is the CD signal in millidegrees, mRw is the mean residue mass (molecular mass in daltons divided by the number of amino acid residues), c is the concentration in milligrams per milliliter, and l is the path length in centimeters. The scan rate was 1.425 s/nm, and three accumulations were conducted for each experiment.

RESULTS

Subdomain IA Comprising Motifs I, Ia, II, and III Is Sufficient for the ATP and DNA Interaction. Previously, we have shown that both ATP and DNA can bind to ADAAD, a proteolytic fragment of SMARCAL1, in the absence of the other ligand. The interaction of ATP with ADAAD induces a conformational change that allows DNA to bind with a higher affinity.[29] Similarly, the interaction of DNA with ADAAD induces a conformational change that allows ATP to bind with a 10-fold higher affinity. As SWI2/SNF2 proteins have been shown to be comprised of two RecA-like domains, we asked which domain is sufficient for the interaction of ATP and DNA in the absence and presence of the other ligand. Binding studies with the deletion construct, MAD47 containing only motifs Q, I, Ia, II, and III of subdomain 1A, showed that this subdomain was sufficient for interaction with ATP in the absence and presence of a saturating concentration of slDNA (Figure 2A–D, Table 1, and Table 3 of the Supporting Information). Similarly, this domain was sufficient for interaction with slDNA in the absence and presence of a saturating concentration of ATP, though the dissociation constant of slDNA in the absence of ATP was 2-fold higher for MAD47 than for the wild type (Figure 2E–H, Table 1, and Table 3 of the Supporting Information). The data, therefore, suggest that subdomain 1A is sufficient for the interaction of ATP and DNA in the absence and presence of the other ligand. Further, the major conformational changes leading to higher affinity binding also appear to occur within this subdomain.

The Conserved Glutamine of Motif Q Regulates the Catalytic Efficiency and the Turnover Number of the ATPase Reaction. The sequence analysis of the SWI2/SNF2 proteins shows that motif Q is present upstream of motif I (Figure 3A). To understand the function of the conserved glutamine residue present in this motif, we mutated the residue to alanine in ADAAD (Figure 3B). As shown in Figure 3C, Q217A showed a complete loss of activity. CD spectroscopy showed that the loss of activity was not due to a loss of global conformation (Figure 3D). This loss of ATPase activity was also not caused by the loss of ATP binding as this ligand was able to bind to the mutant protein in the absence and presence of slDNA with binding constants similar to that of the wild-type protein (Figure 1A–D of the Supporting Information, Table 1 and Table 3 of the Supporting Information). This suggests that the glutamine is required for ATP hydrolysis but not for ATP interaction. Interestingly, the binding constant for the interaction of DNA with the mutant protein was found to be 2-fold higher than that of the wild-type protein (Figure 1E,F of the Supporting Information, Table 1, and Table 3 of the Supporting Information). However, the binding constant for DNA in the presence of a saturating concentration of ATP was found to be similar to that of the wild-type protein (Figure 1G,H of the Supporting Information, Table 1, and Table 3 of the Supporting Information).

To understand whether the presence of the functional group was critical for ATP hydrolysis, glutamine was mutated to asparagine. This mutation did not lead to a loss of ATPase activity (Figure 3C). However, the apparent K_{DNA} was found to be 3-fold higher and the turnover number 1.5-fold higher for the mutant protein than for the wild type (Figure 3E and Table 2). The apparent K_{DNA} was validated using radioactive [^{32}P]-γ-ATP in the ATPase assay (Figure 4A of the Supporting Information). Consequently, the catalytic efficiency was found

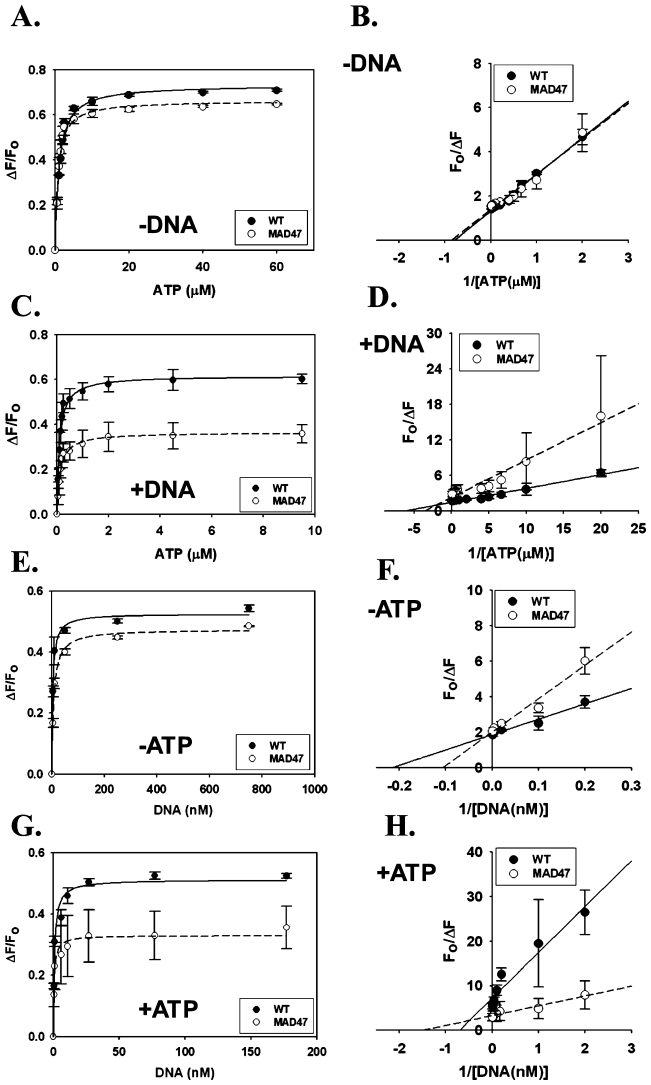

Figure 2. (A) Comparison of ATP binding between ADAAD (●) and MAD47 (○) in the absence of slDNA. The binding data were fit to a one-site saturation model. (B) Double-reciprocal plot analysis of the interaction of ATP with ADAAD (●) and MAD47 (○) in the absence of slDNA. (C) Comparison of ATP binding between ADAAD (●) and MAD47 (○) in the presence of slDNA (2 μM). The binding data were fit to a one-site saturation model. (D) Double-reciprocal plot analysis of the interaction of ATP with ADAAD (●) and MAD47 (○) in the presence of slDNA (2 μM). (E) Comparison of slDNA binding between ADAAD (●) and MAD47 (○) in the absence of ATP. The binding data were fit to a one-site saturation model. (F) Double-reciprocal plot analysis of the interaction of slDNA with ADAAD (●) and MAD47 (○) in the absence of ATP. (G) Comparison of slDNA binding between ADAAD (●) and MAD47 (○) in the absence of ATP (20 μM). The binding data were fit to a one-site saturation model. (H) Double-reciprocal plot analysis of the interaction of slDNA with ADAAD (●) and MAD47 (○) in the presence of ATP (20 μM). In all the experiments, 0.48 μM ADAAD and 0.85 μM MAD47 were used. ADAAD is indicated as WT in the plots.

to be 2-fold lower (Figure 3E and Table 2). These data suggest that Gln 217 is important for DNA binding, and in addition, the shorter length of the side chain of asparagine appears to alter the catalytic efficiency of the mutant by causing a defect in DNA binding. The binding constant for ATP was found to be similar to that of the wild-type protein in the absence and presence of DNA (Figure 1A–D of the Supporting

dx.doi.org/10.1021/bi2014757 | Biochemistry 2012, 51, 3711–3722

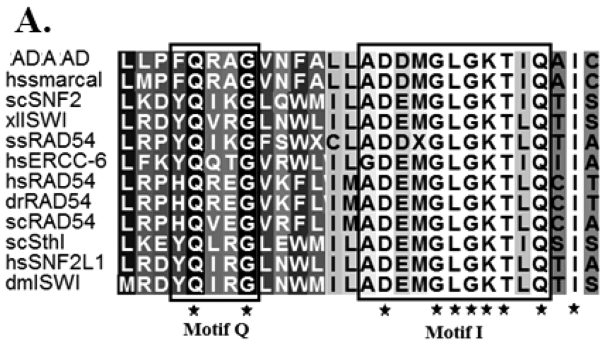

	Organism	Q	D[D,E]MGLGKT
ADAAD	*Bos taurus*	217 aa	235-242 aa
hsSMARCAL1	*Homo sapiens*	440 aa	458-465 aa
scSNF2	*S. cerevisiae*	771 aa	792-799 aa
xlISWI	*Xenopus laevis*	177	198-205 aa
ssRAD54	*Sulfolobus solfatricus*	44	63-70 aa
hsERCC-6	*Homo sapiens*	511	532-539 aa
hsRAD54	*Homo sapiens*	152 aa	183-190 aa
drRAD54	*Danio rerio*	151 aa	180-187 aa
scRAD54	*S. cerevisiae*	275	335-342 aa
scSth1	*S. cerevisiae*	474	495-502 aa
hsSNF2L	*Homo sapiens*	187	208-215 aa
dmISWI	*Drosophila melanogaster*	132	153-160 aa

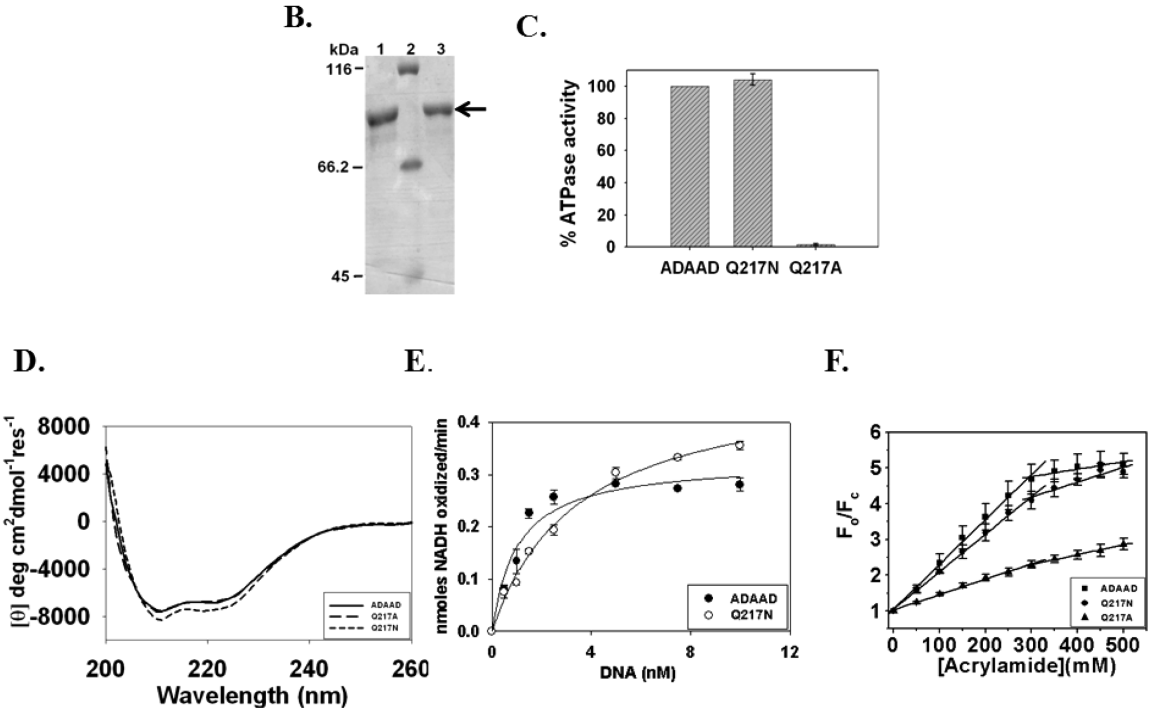

Figure 3. (A) Clustal W analysis of motifs Q and I in SWI2/SNF2 proteins. Gaps were removed prior to identification of the conserved motifs. In ssRad54, the amino acid represented by X is methionine. The amino acid numbers corresponding to these conserved motifs are given in the table. (B) SDS−PAGE showing the purified Q217N and Q217A proteins: lane 1, Q217N; lane 2, molecular mass markers; lane 3, Q217A. (C) Comparison of the ATPase activity of Q217N and Q217A in the presence of slDNA (10 nM) as compared to wild-type ADAAD. The amount of protein used in this experiment was 0.4 μg (97 nM), and the percent ATPase activity was calculated with respect to ADAAD assuming 100% activity for ADAAD. (D) CD spectra of ADAAD, Q217N, and Q217A recorded as explained in Experimental Procedures. (E) ATPase activity of ADAAD and Q217N in the presence of increasing concentrations of slDNA; 1.4 μg (68 nM) of ADAAD (●) or Q217N (○) was incubated at 37 °C for 45 min with increasing concentrations of slDNA in the presence of 2 mM ATP. (F) Stern−Volmer plots were used to analyze the populations of tryptophan present in ADAAD, Q217A, and Q217N. These proteins were titrated in the presence of increasing concentrations of acrylamide, and the fluorescence emission was monitored at 340 nm after excitation at 295 nm.

Table 2. Calculation of Kinetic Parameters for Q217N and Q244A[a]

	K_{DNA} (nM)	V_{DNA} (μmol/min)	k_{cat} (min^{-1})	k_{cat}/K_{DNA} (M^{-1} min^{-1})
wild type	0.9 ± 0.06	0.33 ± 0.001	19.3 ± 0.1	(20.9 ± 1.6) × 10^9
Q217N	3.5 ± 0.02	0.49 ± 0.01	28.7 ± 0.6	(8.23 ± 0.2) × 10^9
Q244A	4.2 ± 0.3	0.26 ± 0.01	15.3 ± 0.4	(3.1 ± 0.2) × 10^9

[a]Each experiment was conducted in duplicate.

Information, Table 1, and Table 3 of the Supporting Information). However, the K_d values for stem−loop DNA in the absence and presence of saturating concentrations of ATP were found to be ~2-fold higher than for the wild-type protein, thus corroborating the increase in the apparent K_{DNA} calculated using ATPase assays (Figure 1E−H of the Supporting Information and Table 1).

Finally, we analyzed the alterations in conformation by acrylamide quenching. We have previously shown that acrylamide quenching can be used to probe conformational changes in ADAAD upon binding to its ligand.[29] The Stern−

dx.doi.org/10.1021/bi2014757 | *Biochemistry* 2012, 51, 3711−3722

Volmer plots obtained clearly indicated a biphasic accessibility of the Trp residues of the ADAAD protein by the quencher, as also previously reported.[29] Similar biphasic plots were obtained in the case of the mutants, as well. However, as one can clearly see from Figure 3F, the slopes of the Stern−Volmer plots were clearly different for the two mutants (Q217A and Q217N) as compared to that of the wild-type protein. The Stern−Volmer parameters obtained from these studies were different from that of wild-type ADAAD in both Q217N and Q217A, suggesting that the conserved glutamine of motif Q is critical for the catalytically competent conformation (Figure 3F and Table 3).

Table 3. Quenching Parameters for ADAAD, Q217N, Q217A, and Q244A in the Absence of ATP and slDNA

	K_{SV1} (M^{-1})	K_{SV2} (M^{-1})	K_a	f_a
ADAAD	12.7 ± 2.0	1.51 ± 0.2	12.7 ± 2.6	0.99
Q217N	10.5 ± 0.8	4.14 ± 0.5	12.8 ± 1.4	0.94
Q217A	4.4 ± 0.5	3.02 ± 0.6	5.5 ± 0.7	0.90
Q244A	9.2 ± 0.2	3.6 ± 0.2	12.3 ± 0.05	0.96

We confirmed that the differences in the K_{SV1} and K_{SV2} parameters were indeed statistically significant using ANCOVA (Table 4 of the Supporting Information). Further, the two sets of populations of tryptophans present in ADAAD and Q217N appear to be more accessible to the quencher than those present in Q217A.

Motif I Is Important for ATP Hydrolysis but Not Ligand Binding. The sequence analysis of motif I from SWI2/SNF2 proteins and the DEAD box helicases reveals interesting differences between the two classes of proteins. The consensus sequence for motif I in the SWI2/SNF2 proteins is [A,G]D[D/E]MGLGKT (Figure 3A), while in the DEAD box helicases, the consensus sequence is AxTGoGKT, where x is either a hydrophilic or a hydrophobic amino acid and o is a hydrophilic amino acid. Further, the SWI2/SNF2 proteins possess a conserved glutamine residue one amino acid downstream of the conserved threonine residue, which is absent in DEAD box helicases. Previously, K241 of ADAAD was shown to be required for ATP hydrolysis but not ATP binding.[29] Here we report the mutation of residues D235, D236, T242, and Q244 to alanine in ADAAD (Figure 4A).

Mutation of D235, D236, and T242 to alanine results in the loss of ATPase activity, suggesting that these residues are essential for catalysis (Figure 4B). CD spectroscopy of D235A and D236A confirmed that the loss of activity was not due to a global loss of structure (Figure 4C). This loss of ATPase activity for all three mutants was also not the result of a loss of ATP binding as the binding constants for ATP in the absence and presence of slDNA were the same as that for the wild-type protein (Figure 2A−D of the Supporting Information, Table 1, and Table 3 of the Supporting Information). Further, the loss of ATP hydrolysis could not be attributed to the loss of DNA binding as D235A and D236A could bind to DNA with the same binding constants as the wild-type protein in the absence and presence of ATP (Figure 2E−H of the Supporting Information). Interestingly, mutating T242 to alanine resulted in 2.4-fold increase in K_d for slDNA in the absence of ATP (Figure 2E,F of the Supporting Information, Table 1, and Table 3 of the Supporting Information). However, the K_d for slDNA in the presence of ATP was the same as that for the wild-type protein (Figure 2G,H of the Supporting Information, Table 1, and Table 3 of the Supporting Information).

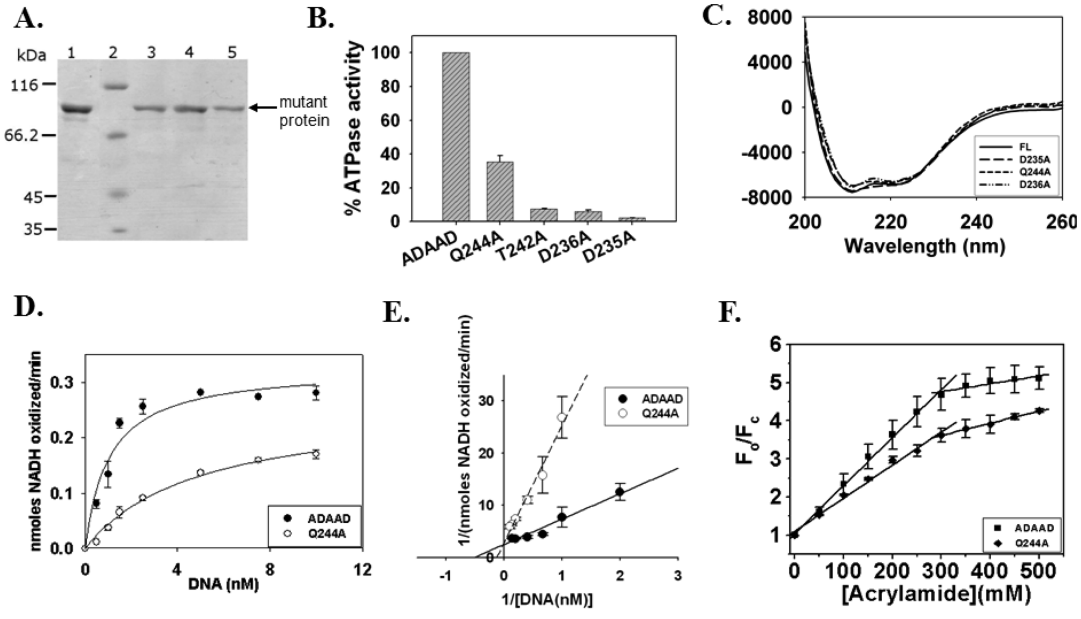

Figure 4. (A) Purified fractions of ADAAD and the site-directed mutants of motif I: lane 1, wild-type ADAAD; lane 2, molecular mass markers; lane 3, Q244A; lane 4, D236A; lane 5, T242A. (B) Comparison of ATPase activities of D235A, D236A, T242A, and Q244A with respect to that of wild-type ADAAD. The concentrations of DNA and ATP used in the reaction were 10 nM and 2 mM, respectively. The percent ATPase activity of the mutants was calculated with respect to that of the wild-type protein. (C) CD spectra of D235A, D236A, and Q244A were recorded as explained in Experimental Procedures. FL indicates ADAAD. (D) Kinetic analysis of ATP hydrolysis mediated by Q244A. Purified ADAAD (●) or Q244A (○) (1.4 μg, 68 nM) was incubated at 37 °C for 45 min with increasing concentrations of slDNA in the presence of 2 mM ATP. The data were fit to the Michealis−Menten equation. (E) The same data fit to Lineweaver−Burk equation show that the V_{DNA} was the same for ADAAD (●) and Q244A (○), while the K_{DNA} was different. (F) Stern−Volmer plots show that the accessibility of tryptophan residues to acrylamide was different in ADAAD and Q244A.

dx.doi.org/10.1021/bi2014757 | *Biochemistry* 2012, 51, 3711−3722

Q244A Regulates the Catalytic Efficiency but Is Not Required for ATP Hydrolysis. The SWI2/SNF2 proteins contain a conserved glutamine one amino acid after the threonine of the GKT box. Mutation of Q244 to alanine resulted in a 60% loss of ATPase activity (Figure 4B) but led to no major global conformational change in the protein (Figure 4C). Kinetic analysis showed that the apparent K_{DNA} was 4-fold higher than that of the wild-type protein, while the V_{DNA} was the same (Figure 4D,E and Table 2). The apparent K_{DNA} was validated using radioactive [^{32}P]-γ-ATP in the ATPase assay (Figure 4B of the Supporting Information). Furthermore, the k_{cat} was the same as that of the wild-type protein, suggesting that the turnover number was not affected. However, the catalytic efficiency was 5-fold lower (Figure 4D and Table 2). Analysis of the binding constants showed that the interaction of ATP with Q244A in the absence and presence of slDNA was the same as that of the wild-type protein (Figure 3A–D of the Supporting Information, Table 1, and Table 3 of the Supporting Information). The K_d for the interaction of slDNA in the absence of ATP with Q244A was found to be 2.5-fold higher than that with the wild-type protein (Figure 3E,F of the Supporting Information, Table 1, and Table 3 of the Supporting Information). However, the K_d for the interaction of slDNA with Q244A in the presence of ATP was the same as that of the wild-type protein (Figure 3G,H of the Supporting Information, Table 1, and Table 3 of the Supporting Information).

The conformation of Q244A was further analyzed by acrylamide quenching of tryptophan fluorescence and the Stern–Volmer plots obtained (Figure 4F and Table 3). As one can see clearly from Figure 4F, Q244A exhibited significant differences in the access of the quencher to the Trp residues, clearly suggesting that despite conservation of the overall global fold, there were subtle differences in the conformation of the mutant versus the ADAAD that could have implications for the catalytic activity of the protein.

The Adenine Moiety of ATP Is Sufficient for the Interaction of the Ligand with the Protein. Crystal structure studies have shown that ATP binding with helicases occurs through the interactions of the phosphate group of ATP with the lysine of the GKT box.[12,32,33] In addition, the crystal structure of eIF4A has shown that the glutamine residue of the Q motif also makes contacts with the N6 and N7 positions of the adenine ring of the nucleotide.[34] However, our binding studies show that neither motif Q nor motif I of ADAAD is required for interaction with ATP. Therefore, we sought to understand how ATP binds to the protein.

Binding studies with ADP showed that the binding constant for the interaction of ADP with ADAAD in the absence of slDNA was similar to that of ATP (Figure 5A; K_d = 1.4 ± 0.1 μM). As ATP contains an adenine ring, the interaction of adenine with ADAAD was assessed. Binding studies showed that the binding constant for the interaction of adenine in the absence of DNA with ADAAD was similar to that of ATP interaction (Figure 5B and Table 4).

To understand whether the adenine ring was sufficient for the interaction in the presence of slDNA, binding studies were conducted after saturating ADAAD with slDNA. As shown in Figure 5C, saturating the protein with slDNA leads to a 10-fold increase in the binding affinity for adenine, suggesting that the adenine ring is sufficient for both low-affinity and high-affinity interaction with the protein (Figure 5C and Table 4).

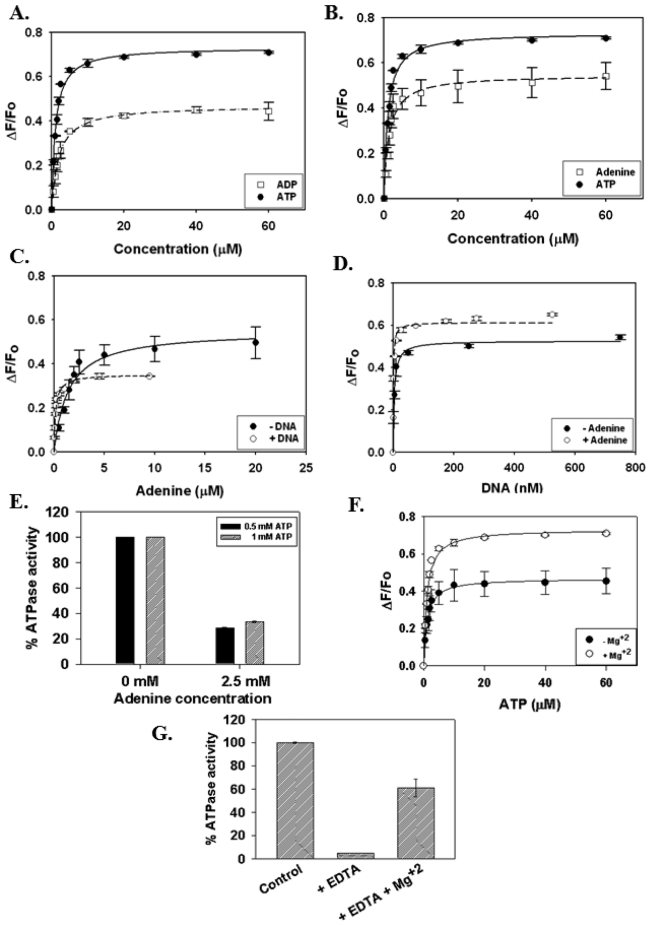

Figure 5. (A) Comparison of the interaction of ATP (●) and ADP with ADAAD (□) in the absence of slDNA. (B) Comparison of the interaction of ATP (●) and adenine (□) with ADAAD in the absence of slDNA. (C) Comparison of the interaction of adenine with ADAAD in the absence (●) and presence (○) of slDNA (2 μM). (D) Comparison of the interaction of slDNA with ADAAD in the absence (●) and presence (○) of adenine (20 μM). (E) Inhibition of ATPase activity by adenine. ADAAD (0.9 μg, 0.22 μM) was incubated with 10 nM slDNA and ATP in the absence or presence of 2.5 mM adenine for 1 h. The experiment was conducted at two different ATP concentrations (0.5 and 1.0 mM). (F) Comparison of the interaction of ATP in the absence (●) and presence (○) of Mg^{2+}. ADAAD (0.6 μM) was titrated with ATP in the presence of REG buffer either lacking Mg^{2+} or containing 1 mM Mg^{2+}. (G) Mg^{2+} is required for ATP hydrolysis. ATPase assays were conducted using ADAAD in the presence of REG buffer containing 1 mM Mg^{2+}. The ATPase activity was lost when 5 mM EDTA was added to the reaction mixture. The activity was restored when 10 mM Mg^{2+} was added to the reaction mixture containing 5 mM EDTA. In all cases, ADAAD (0.3 μg, 73 nM) was used and the reaction was conducted in the presence of REG buffer containing 1 mM Mg^{2+}.

The interaction of ATP with ADAAD induces a change in conformation that allows DNA to bind with a higher affinity.[29] To understand whether the adenine ring can induce a similar conformation change, ADAAD was saturated with adenine and the binding of slDNA was monitored. As shown in Figure 5D, the adenine ring itself was sufficient to allow slDNA to bind with a higher affinity (Figure 5D and Table 4).

If the adenine ring were sufficient for the interaction, then adenine would be able to act as an inhibitor of ATP binding. ATPase assays confirmed that addition of a 2.5-fold excess of

dx.doi.org/10.1021/bi2014757 | Biochemistry 2012, 51, 3711–3722

Table 4. Binding Parameters for the Interaction of Adenine and ADP with ADAAD

	K_d (M)		
	nucleotide in the absence of slDNA	nucleotide in the presence of slDNA	slDNA in the presence of the nucleotide
ATP	$(1.5 \pm 0.1) \times 10^{-6}$	$(0.14 \pm 0.02) \times 10^{-6}$	$(0.8 \pm 0.03) \times 10^{-9}$
adenine	$(1.35 \pm 0.1) \times 10^{-6}$	$(0.16 \pm 0.01) \times 10^{-6}$	$(1.2 \pm 0.09) \times 10^{-9}$

adenine indeed was able to inhibit the activity of the protein (Figure 5E).

Mg^{2+} Is Required for Catalysis but Not for Interaction of the Protein with ATP. A corollary of the conclusion given above is that Mg^{2+} ions should not be required for interaction of ATP with the protein as these ions are expected to primarily coordinate interaction of the phosphate groups of ATP with the protein. To test this hypothesis, we studied the interaction of ATP with ADAAD in the absence of Mg^{2+} ions. As shown in Figure 4F, the binding constant for the interaction of ATP with the protein in the absence of Mg^{2+} ions (K_d = 1.14 ± 0.28 μM) mimics the binding constant for the interaction that occurs in the presence of Mg^{2+}, suggesting that the Mg^{2+} ions are dispensable for the interaction. However, Mg^{2+} ions are required for ATP hydrolysis as evidenced by the loss of ATP hydrolysis when 5 mM EDTA was added to the ATPase reaction (Figure 5G). The ATPase activity was restored when additional 10 mM Mg^{2+} was present in the reaction mixture (Figure 5G).

As further proof, ADAAD was found to interact with TNP-ATP in the absence of Mg^{2+} (Figure 4C,D of the Supporting Information).

The γ-Phosphate of ATP Is Required for Inducing Conformational Change in ADAAD, Making It Competent for ATP Hydrolysis. If the adenine ring is sufficient for the interaction, what is the role of the phosphate residues? As ATPase activity is observed only in the presence of ATP, it is clear that the γ-phosphate of ATP is a deciding factor for the catalytic function of the protein. Hence, we studied the conformation of the protein using CD to understand the importance of ATP in the interaction. CD spectroscopy showed that the conformations induced by adenine and ADP binding are different from that induced by ATP binding, suggesting a role for the γ-phosphate in generating the ATPase activity-competent conformation of the protein (Figure 6A).

The conformation of the protein in the presence of adenine, ADP, or ATP, in combination with slDNA, was further studied using CD spectroscopy. The conformation of the protein in the presence of ATP and DNA was found to be indeed different from the conformation of the protein in the presence of either ADP and DNA or adenine and DNA, confirming once again that the γ-phosphate is required for inducing the ATPase-competent conformation (Figure 6B).

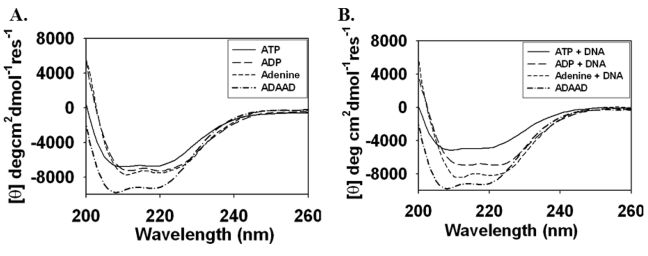

Figure 6. (A) CD spectra of ADAAD in the presence of ATP, ADP, and adenine recorded in the absence of slDNA as explained in Experimental Procedures. The conformation of ATP-bound ADAAD is different from the ADP- and adenine-bound conformations, indicating the importance of γ-phosphate. (B) CD spectra of ADAAD in the presence of ATP, ADP, and adenine in the presence of 2 μM slDNA recorded as explained in Experimental Procedures. In all these experiments, 1.2 μM ADAAD and 20 μM nucleotide were used.

The Interaction with ATP via the Adenine Ring Is a Characteristic Feature of the SWI2/SNF2 Proteins. On the basis of the conservation of the helicase motifs among the SWI2/SNF2 proteins, we hypothesized that these proteins, in general, bind ATP via the adenine ring. To prove the hypothesis, we cloned and overexpressed Sth1 (amino acids 288−1359) from *S. cerevisiae* as His-tagged protein in *E. coli*.[21] His-tagged Sth1 was purified as explained in Experimental Procedures (Figure 7A). The interaction of the purified protein with ATP and adenine in the presence and absence of Mg^{2+} was studied using fluorescence spectroscopy. As shown in Figure 7B, ATP bound to Sth1 with a K_d of 1.5 ± 0.5 μM in the presence of Mg^{2+}, while the K_d for the interaction in the absence of Mg^{2+} was 1.4 ± 0.7 μM. Sth1 was also able to interact with adenine with a K_d of 1.3 ± 0.3 μM, suggesting that the SWI2/SNF2 proteins in general interact with ATP via the adenine ring.

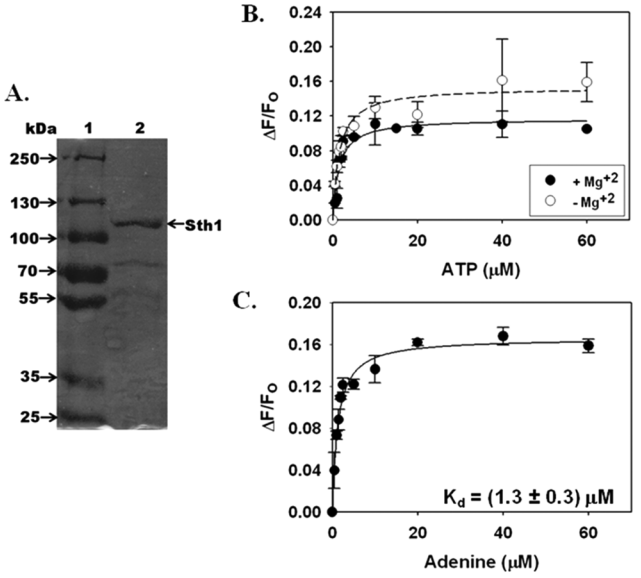

Figure 7. ATP interacts with SWI2/SNF2 proteins via the adenine ring. (A) His-tagged Sth1 was purified from *E. coli*: lane 1, molecular mass markers; lane 2, purified Sth1. (B) Sth1 binds to ATP in the presence and absence of Mg^{2+}. The K_d for ATP in the presence of Mg^{2+} was 1.5 ± 0.5 μM and in the absence of Mg^{2+} was 1.4 ± 0.4 μM. (C) Sth1 binds to adenine with a K_d similar to that of ATP, suggesting that the interaction of ATP with SWI2/SNF2 proteins occurs via the adenine ring.

dx.doi.org/10.1021/bi2014757 | *Biochemistry* 2012, 51, 3711−3722

DISCUSSION

The SF2 class of helicases comprise DEAD box RNA helicases and the SWI2/SNF2 family of chromatin remodeling proteins.[5] Both the DEAD box RNA helicases and the SWI2/SNF2 family proteins possess the seven helicase motifs.[5,35] In addition, both classes of proteins possess the Q motif.[6] These motifs have been shown to be necessary and sufficient for ATP hydrolysis.[28] The role of each individual motif has been delineated in DEAD box RNA helicases but not in SWI2/SNF2 proteins.[17] In this work, we seek to characterize the function of motif Q and I with respect to DNA binding, ATP binding, and ATP hydrolysis using ADAAD, a proteolytic fragment of SMARCAL1, a member of the SWI2/SNF2 protein family. Our studies highlight important differences between RNA helicases and SWI2/SNF2 proteins, both of which belong to the SF2 family of helicases. We believe these differences have a bearing on the functions of these two important families of proteins.

Our studies indicate that both motif Q and motif I of the SWI2/SNF2 proteins are important for catalysis but not for ATP binding. The role of motif I, the classical Walker A box, has been a conundrum. In some helicases, like in UvrD, eIF4A, and primase/helicase of bacteriophage, this motif has been shown to be important both for catalysis and for ATP binding.[11,12,36] In contrast, in other helicases, including RAD3, this motif has been primarily identified as being critical for catalysis.[37] From our studies, it is evident that in ADAAD and possibly in SWI2/SNF2 proteins, motif I is required for catalysis but not for ATP binding.

Motif Q was discovered by Tanner et al., and the glutamine residue is highly conserved in DEAD box RNA helicases.[6] Glutamine has been shown to make contacts with the N6 and N7 positions of the adenine base of the ATP in DEAD box proteins.[14] Further, mutating the conserved glutamine of motif Q to alanine in Ded1 protein has been shown to result in lowered catalytic efficiency as well as reduced affinity for ATP.[14] In ADAAD, as in all SWI2/SNF2 proteins, a conserved glutamine is found ~17 amino acids upstream of motif I. Mutating Q217 in ADAAD to alanine resulted in a complete loss of ATPase activity without affecting ATP binding. However, this mutant showed impaired DNA binding in the absence of ATP. Furthermore, mutating Q217 to asparagine resulted in higher turnover numbers yet lowered the catalytic efficiency because of a defect in K_{DNA} as assessed by the enzyme assays. This was also supported by higher K_d values for DNA binding in the Q217N mutant, suggesting that the primary role of Q217 could be at the level of DNA binding. Thus, the function of both motif Q and motif I appears to be at variance from that in other SF2 helicases.

The SWI2/SNF2 proteins, in addition, contain a conserved glutamine one amino acid after the threonine of the GKT box. This glutamine regulates the catalytic efficiency of the protein but not the turnover number.

Interestingly, Q217, T242, and Q244 also appear to be important for the interaction with DNA in the absence of ATP because mutating these residues results in an alteration of the K_d (~2-fold) for DNA. However, this defect is compensated for in the presence of ATP, because there appears to be no significant difference in the affinity for DNA for any of these mutants in the presence of ATP.

Q217A and Q244A exhibit impaired catalytic efficiency. In our earlier paper, we showed that it was slDNA and not ATP that dictated the conformation of the protein, and using a set of four theoretical models, we showed that the one most likely applicable to ADAAD involves binding of the slDNA to ADAAD first followed by binding of ATP to the protein−DNA complex and its hydrolysis.[29] Our current results in the framework of this model would imply that the defect in DNA binding would indeed be reflected in a weaker K_{DNA} for the catalytic process without altering its k_{cat} values.

How does ATP bind? In SWI2/SNF2 proteins, the interaction appears to be primarily mediated via the adenine ring in the absence and presence of DNA. This is unlike the situation in other SF1 helicases and SF2 helicases containing the DEAD motif. For example, in Rep helicase, ATP has been shown to bind at least 10^6-fold tighter than adenosine.[38] Similarly, differences in the affinity for ADP and ATP have been shown in the case of DbpA, a RNA helicase in which ADP has been shown to bind with a higher affinity than ATP.[39] In ADAAD, the adenine ring also appears to be sufficient to induce the conformational change required for the high-affinity interaction of DNA with the protein. This is similar to the observation in some of the DExH motif-containing helicases. For example, DHX9 that contains the DEIH motif has been shown to bind to ADP, GDP, and CDP.[40] Similarly, Prp4, a DEAH motif-containing protein, has not been shown to possess the ability to discriminate between the various nucleotides.[41] This inability to discriminate between nucleotides is due to the differences in the manner in which the proteins bind the nucleotide. In both PcrA and Rep helicases, both of which are SF1, the crystal structure shows that residues of both motifs I and VI are involved in interacting with ADP.[32,42] In SF2 helicases containing the DEAD box proteins, the conserved glutamine of motif Q has been shown to interact with the adenine ring.[40] The situation changes when we consider the DExH motif-containing proteins, where the adenine base is not specifically recognized. In Mtr4, a DExH helicase from *S. cerevisiae*, the adenine ring has been shown to be sandwiched between Arg 547 and Phe 148, even though N6 of the adenine ring makes contacts with the conserved glutamine of motif Q.[43] Similarly, in Prp34, a DEAH helicase, the ADP molecule has been shown to be sandwiched between the two RecA domains, with the adenine ring stacked between Arg 159 of motif Ia and Phe 359.[41] In addition, conserved residues from motifs IV and V make contacts with the ribose ring, while Ser 155 and Gln 354 are involved in making hydrogen bonds with the adenine via water molecules.[41] Thus, it is quite possible that also in ADAAD multiple amino acids are involved in coordinating the interaction with the adenine base.

Experimental data suggest that in ADAAD the γ-phosphate of ATP is required only for inducing the ATPase-competent conformation. This is similar to what has been reported for CopB ATPase, a P-type ATPase.[44] The base/sugar part of ATP has been shown to dictate the binding constants for the interaction. Further, the authors have shown that the γ-phosphate makes a transient contact with a conserved aspartate located in the phosphorylation domain of the protein.[44] It is, therefore, possible that the interaction of ATP with ADAAD follows a principle similar to that of CopB ATPase.

It is interesting to note that even though the SWI2/SNF2 proteins have been classified, on the basis of sequence homology, as SF2 helicases they appear to behave more like P-type ATPases. Additional experiments are currently underway to delineate the region of interaction for ATP as well as for DNA and to elucidate the conformational changes induced upon binding of the γ-phosphate of ATP.

■ ASSOCIATED CONTENT

Supporting Information

Sequences of primers as well as the PCR conditions used for creating site-directed mutagenesis (Tables 1 and 2, respectively), K_d values calculated using double-reciprocal plots (Table 3), ANCOVA results (Table 4), binding data for all the mutants (Figures 1−3), and ATPase assays using radioactive [^{32}P]-γ-ATP as well as interaction of ADAAD with TNP-ATP (Figure 4). This material is available free of charge via the Internet at http://pubs.acs.org.

■ AUTHOR INFORMATION

Corresponding Author

*Room 333, School of Life Sciences, JNU, New Delhi 110067, India. E-mail: rohini_m@mail.jnu.ac.in. Telephone: +91 11 26704154. Fax: +91 11 2671758.

Present Address

†Department of Biotechnology and Bioinformatics, North-Eastern Hill University, Shillong, Meghalaya, India.

Author Contributions

M.N. and M.G. contributed equally to this paper.

Funding

This work was supported by grants from the Defense Research and Development Organisation (DRDO), DST-PURSE, and UGC resource networking to R.M. M.N. acknowledges the fellowship granted by the Department of Biotechnology, while M.G. was supported by a fellowship from the Council for Scientific and Industrial Research.

Notes

The authors declare no competing financial interest.

■ ACKNOWLEDGMENTS

We gratefully acknowledge the technical help provided by Deepak Kumar Jha, Vidhi Mathur, Shashi Gupta, and Nimish Khanna.

■ REFERENCES

(1) van Attikum, H., and Gasser, S. M. (2005) ATP-dependent chromatin remodeling and DNA double-strand break repair. *Cell Cycle 4*, 1011−1014.

(2) Hur, S.-K., Park, E.-J., Han, J.-E., Kim, Y.-A., Kim, J.-D., Kang, D., and Kwon, J. (2010) Roles of human INO80 chromatin remodeling enzyme in DNA replication and chromosome segregation suppress genome instability. *Cell. Mol. Life Sci. 67*, 2283−2296.

(3) Clapier, C. R., and Cairns, B. R. (2009) The biology of chromatin remodeling complexes. *Annu. Rev. Biochem. 78*, 273−304.

(4) Trotter, K. W., and Archer, T. K. (2008) The BRG1 transcriptional coregulator. *Nucl. Recept. Signaling 6*, e004.

(5) Gorbalenya, A. E., and Koonin, E. V. (1993) Helicases: Amino acid sequence comparisons and structure-function relationships. *Curr. Opin. Struct. Biol. 3*, 419−429.

(6) Tanner, N. K., Cordin, O., Banroques, J., Doère, M., and Linder, P. (2003) The Q motif: A newly identified motif in DEAD box helicases may regulate ATP binding and hydrolysis. *Mol. Cell 11*, 127−138.

(7) Thomä, N. H., Czyzewski, B. K., Alexeev, A. A., Mazin, A. V., Kowalczykowski, S. C., and Pavletich, N. P. (2005) Structure of the SWI2/SNF2 chromatin-remodeling domain of eukaryotic Rad54. *Nat. Struct. Mol. Biol. 12*, 350−356.

(8) Dürr, H., Körner, C., Müller, M., Hickmann, V., and Hopfner, K.-P. (2005) X-ray structures of the *Sulfolobus solfataricus* SWI2/SNF2 ATPase core and its complex with DNA. *Cell 121*, 363−373.

(9) Shaw, G., Gan, J., Zhou, Y. N., Zhi, H., Subburaman, P., Zhang, R., Joachimiak, A., Jin, D. J., and Ji, X. (2008) Structure of RapA, a Swi2/Snf2 protein that recycles RNA polymerase during transcription. *Structure 16*, 1417−1427.

(10) Dürr, H., Flaus, A., Owen-Hughes, T., and Hopfner, K.-P. (2006) Snf2 family ATPases and DExx box helicases: Differences and unifying concepts from high-resolution crystal structures. *Nucleic Acids Res. 34*, 4160−4167.

(11) Sinha, K. M., Glickman, M. S., and Shuman, S. (2009) Mutational analysis of *Mycobacterium* UvrD1 identifies functional groups required for ATP hydrolysis, DNA unwinding, and chemo-mechanical coupling. *Biochemistry 48*, 4019−4030.

(12) Rozen, F., Pelletier, J., Trachsel, H., and Sonenberg, N. (1989) A lysine substitution in the ATP-binding site of eucaryotic initiation factor 4A abrogates nucleotide-binding activity. *Mol. Cell. Biol. 9*, 4061−4063.

(13) Soultanas, P., Dillingham, M. S., Velankar, S. S., and Wigley, D. B. (1999) DNA binding mediates conformational changes and metal ion coordination in the active site of PcrA helicase. *J. Mol. Biol. 290*, 137−148.

(14) Cordin, O., Tanner, N. K., Doère, M., Linder, P., and Banroques, J. (2004) The newly discovered Q motif of DEAD-box RNA helicases regulates RNA-binding and helicase activity. *EMBO J. 23*, 2478−2487.

(15) Papanikou, E., Karamanou, S., Baud, C., Sianidis, G., Frank, M., and Economou, A. (2004) Helicase motif III in SecA is essential for coupling preprotein binding to translocation ATPase. *EMBO Rep. 5*, 807−811.

(16) Dillingham, M. S., Soultanas, P., and Wigley, D. B. (1999) Site-directed mutagenesis of motif III in PcrA helicase reveals a role in coupling ATP hydrolysis to strand separation. *Nucleic Acids Res. 27*, 3310−3317.

(17) Cordin, O., Banroques, J., Tanner, N. K., and Linder, P. (2006) The DEAD-box protein family of RNA helicases. *Gene 367*, 17−37.

(18) Pause, A., Méthot, N., and Sonenberg, N. (1993) The HRIGRXXR region of the DEAD box RNA helicase eukaryotic translation initiation factor 4A is required for RNA binding and ATP hydrolysis. *Mol. Cell. Biol. 13*, 6789−6798.

(19) Laurent, B. C., Treich, I., and Carlson, M. (1993) Role of yeast SNF and SWI proteins in transcriptional activation. *Cold Spring Harbor Symp. Quant. Biol. 58*, 257−263.

(20) Khavari, P. A., Peterson, C. L., Tamkun, J. W., Mendel, D. B., and Crabtree, G. R. (1993) BRG1 contains a conserved domain of the SWI2/SNF2 family necessary for normal mitotic growth and transcription. *Nature 366*, 170−174.

(21) Du, J., Nasir, I., Benton, B. K., Kladde, M. P., and Laurent, B. C. (1998) Sth1p, a *Saccharomyces cerevisiae* Snf2p/Swi2p homolog, is an essential ATPase in RSC and differs from Snf/Swi in its interactions with histones and chromatin-associated proteins. *Genetics 150*, 987−1005.

(22) Richmond, E., and Peterson, C. L. (1996) Functional analysis of the DNA-stimulated ATPase domain of yeast SWI2/SNF2. *Nucleic Acids Res. 24*, 3685−3692.

(23) Boerkoel, C. F., Takashima, H., John, J., Yan, J., Stankiewicz, P., Rosenbarker, L., André, J.-L., Bogdanovic, R., Burguet, A., Cockfield, S., Cordeiro, I., Fründ, S., Illies, F., Joseph, M., Kaitila, I., Lama, G., Loirat, C., McLeod, D. R., Milford, D. V., Petty, E. M., Rodrigo, F., Saraiva, J. M., Schmidt, B., Smith, G. C., Spranger, J., Stein, A., Thiele, H., Tizard, J., Weksberg, R., Lupski, J. R., and Stockton, D. W. (2002) Mutant chromatin remodeling protein SMARCAL1 causes Schimke immuno-osseous dysplasia. *Nat. Genet. 30*, 215−220.

(24) Van Houdt, J. K. J., Nowakowska, B. A., Sousa, S. B., van Schaik, B. D. C., Seuntjens, E., Avonce, N., Sifrim, A., Abdul-Rahman, O. A., van den Boogaard, M.-J. H., Bottani, A., Castori, M., Cormier-Daire, V., Deardorff, M. A., Filges, I., Fryer, A., Fryns, J.-P., Gana, S., Garavelli, L., Gillessen-Kaesbach, G., Hall, B. D., Horn, D., Huylebroeck, D., Klapecki, J., Krajewska-Walasek, M., Kuechler, A., Lines, M. A., Maas, S., MacDermot, K. D., McKee, S., Magee, A., de Man, S. A., Moreau, Y., Morice-Picard, F., Obersztyn, E., Pilch, J., Rosser, E., Shannon, N., Stolte-Dijkstra, I., Van Dijck, P., Vilain, C., Vogels, A., Wakeling, E., Wieczorek, D., Wilson, L., Zuffardi, O., van Kampen, A. H. C.,

Devriendt, K., Hennekam, R., and Vermeesch, J. R. (2012) Heterozygous missense mutations in SMARCA2 cause Nicolaides-Baraitser syndrome. *Nat. Genet. 44*, 445−449.
(25) Mesner, L. D., Sutherland, W. M., and Hockensmith, J. W. (1991) DNA-dependent adenosine triphosphatase A is the eukaryotic analogue of the bacteriophage T4 gene 44 protein: Immunological identity of DNA replication-associated ATPases. *Biochemistry 30*, 11490−11494.
(26) Mesner, L. D., Truman, P. A., and Hockensmith, J. W. (1993) DNA-dependent adenosinetriphosphatase A: Immunoaffinity purification and characterization of immunological reagents. *Biochemistry 32*, 7772−7778.
(27) Hockensmith, J. W., Wahl, A. F., Kowalski, S., and Bambara, R. A. (1986) Purification of a calf thymus DNA-dependent adenosinetriphosphatase that prefers a primer-template junction effector. *Biochemistry 25*, 7812−7821.
(28) Muthuswami, R., Truman, P. A., Mesner, L. D., and Hockensmith, J. W. (2000) A eukaryotic SWI2/SNF2 domain, an exquisite detector of double-stranded to single-stranded DNA transition elements. *J. Biol. Chem. 275*, 7648−7655.
(29) Nongkhlaw, M., Dutta, P., Hockensmith, J. W., Komath, S. S., and Muthuswami, R. (2009) Elucidating the mechanism of DNA-dependent ATP hydrolysis mediated by DNA-dependent ATPase A, a member of the SWI2/SNF2 protein family. *Nucleic Acids Res. 37*, 3332−3341.
(30) King, E. J. (1932) The colorimetric determination of phosphorus. *Biochem. J. 26*, 292−297.
(31) Gawronski, J. D., and Benson, D. R. (2004) Microtiter assay for glutamine synthetase biosynthetic activity using inorganic phosphate detection. *Anal. Biochem. 327*, 114−118.
(32) Subramanya, H. S., Bird, L. E., Brannigan, J. A., and Wigley, D. B. (1996) Crystal structure of a DExx box DNA helicase. *Nature 384*, 379−383.
(33) Kim, J. L., Morgenstern, K. A., Griffith, J. P., Dwyer, M. D., Thomson, J. A., Murcko, M. A., Lin, C., and Caron, P. R. (1998) Hepatitis C virus NS3 RNA helicase domain with a bound oligonucleotide: The crystal structure provides insights into the mode of unwinding. *Structure 6*, 89−100.
(34) Benz, J., Trachsel, H., and Baumann, U. (1999) Crystal structure of the ATPase domain of translation initiation factor 4A from *Saccharomyces cerevisiae*: The prototype of the DEAD box protein family. *Structure 7*, 671−679.
(35) Pyle, A. M. (2008) Translocation and unwinding mechanisms of RNA and DNA helicases. *Annu. Rev. Biophys. 37*, 317−336.
(36) Pause, A., and Sonenberg, N. (1992) Mutational analysis of a DEAD box RNA helicase: The mammalian translation initiation factor eIF-4A. *EMBO J. 11*, 2643−2654.
(37) Sung, P., Higgins, D., Prakash, L., and Prakash, S. (1988) Mutation of lysine-48 to arginine in the yeast RAD3 protein abolishes its ATPase and DNA helicase activities but not the ability to bind ATP. *EMBO J. 7*, 3263−3269.
(38) Moore, K. J., and Lohman, T. M. (1994) Kinetic mechanism of adenine nucleotide binding to and hydrolysis by the *Escherichia coli* Rep monomer. 2. Application of a kinetic competition approach. *Biochemistry 33*, 14565−14578.
(39) Talavera, M. A., and De La Cruz, E. M. (2005) Equilibrium and kinetic analysis of nucleotide binding to the DEAD-box RNA helicase DbpA. *Biochemistry 44*, 959−970.
(40) Högbom, M., Collins, R., van den Berg, S., Jenvert, R.-M., Karlberg, T., Kotenyova, T., Flores, A., Karlsson Hedestam, G. B., and Schiavone, L. H. (2007) Crystal structure of conserved domains 1 and 2 of the human DEAD-box helicase DDX3X in complex with the mononucleotide AMP. *J. Mol. Biol. 372*, 150−159.
(41) He, Y., Andersen, G. R., and Nielsen, K. H. (2010) Structural basis for the function of DEAH helicases. *EMBO Rep. 11*, 180−186.
(42) Korolev, S., Hsieh, J., Gauss, G. H., Lohman, T. M., and Waksman, G. (1997) Major domain swiveling revealed by the crystal structures of complexes of *E. coli* Rep helicase bound to single-stranded DNA and ADP. *Cell 90*, 635−647.
(43) Weir, J. R., Bonneau, F., Hentschel, J., and Conti, E. (2010) Structural analysis reveals the characteristic features of Mtr4, a DExH helicase involved in nuclear RNA processing and surveillance. *Proc. Natl. Acad. Sci. U.S.A. 107*, 12139−12144.
(44) Völlmecke, C., Kötting, C., Gerwert, K., and Lübben, M. (2009) Spectroscopic investigation of the reaction mechanism of CopB-B, the catalytic fragment from an archaeal thermophilic ATP-driven heavy metal transporter. *FEBS J. 276*, 6172−6186.